

Off-Fermi Shell Nucleons in Superdense Asymmetric Nuclear Matter

Michael McGauley^a and Misak M. Sargsian^b

^a *Miami Dade College, Miami, FL 33176, USA*

^b *Department of Physics, Florida International University, Miami, FL 33199 USA*

(Dated: October 3, 2018)

Recent observations of the strong dominance of proton-neutron (pn) relative to pp and nn short-range correlations (SRCs) in nuclei indicate on possibility of unique new condition for asymmetric high density nuclear matter, in which the pp and nn interactions are suppressed while the pn interactions are enhanced due to tensor interaction. We demonstrate that for sufficiently asymmetric case and high densities the momentum distribution of the smaller p -component is strongly deformed with protons increasingly populating the momentum states beyond the Fermi surface. This result is obtained by extracting the probabilities of two-nucleon (2N) SRCs from the analysis of the experimental data on high momentum transfer inclusive electro-nuclear reactions. We fitted the extracted probabilities as a function of nuclear density and asymmetry and used the fit to estimate the fractions of the off-Fermi shell nucleons in the superdense nuclear matter relevant to neutron stars. Our results indicate that starting at *three* nuclear saturation densities the protons with fractional densities $\frac{1}{9}$ will populate mostly the high momentum tail of the momentum distribution while only 2% of the neutrons will do so. We discuss the implications of this condition for neutron stars and emphasize that it may be characteristic to any asymmetric two component Fermi system with suppressed central and enhanced short-range tensor interactions between the two components.

The recent experiments on high-momentum transfer semiexclusive reactions[1, 2] in which the struck nucleon from the nucleus is detected in coincidence with the recoil nucleon from SRC, found striking disbalance between pn and pp/nn correlations. They found that protons struck from the nucleus with initial momenta of $k_F < p \leq 600$ MeV/c, in the 92% of the time emerge from the pn SRC, while the pp and nn SRCs are significantly suppressed, contributing only $\approx 4\%$ to the high momentum part of the nucleon momentum distribution in nuclei. This disbalance was understood based on the dominance of the NN tensor interaction in the $300 < p \leq 600$ MeV/c momentum range relevant to 2N SRCs in nuclei[1, 3, 4]. The tensor-interaction dominance is due to the fact that in this momentum range corresponding to inter-nucleon distances of ~ 1 Fm the NN central potential is crossing the zero due to transition from attractive to the repulse interactions. As a result at these distances overall NN potential is dominated by tensor interaction, which results to the suppression of s -channel isostriplet pp and nn interactions and enhancement of the interaction in isosinglet, $L=2$, pn channel. The resulting picture for the nuclear matter consisting of protons and neutrons at densities in which inter-nucleon distances are ~ 1 Fm is rather unique: it represents a system with suppressed pp and nn but enhanced pn interactions.

The goal of the present study is to understand how the high momentum part of the momentum distributions of protons and neutrons are defined in the high density nuclear matter under the above described conditions.

New Relation between High Momentum p - and n -distributions in Nuclei: Due to short range nature of NN interaction the nuclear momentum distribution, $n^A(p)$, for momenta, p , exceeding the characteristic nuclear Fermi momentum k_F is predominantly defined

by the momentum distribution in the SRCs. There is a rather large experimental body of information indicating that for the range of $k_F < p \leq 600$ MeV/c the SRCs are dominated by 2N correlations, which consist of mainly the pn pairs (for recent reviews see [11, 12]).

In recent work[13] based on the dominance of the pn SRCs we predicted two new properties for the nuclear momentum distributions at $\sim k_F < p < 600$: (i) There is an approximate equality of p - and n - momentum distributions weighted by their relative fractions in the nucleus $x_p = \frac{Z}{A}$ and $x_n = \frac{A-Z}{A}$:

$$x_p n_p^A(p) \approx x_n n_n^A(p), \quad (1)$$

with $\int n_{p/n}^A(p) d^3p = 1$. (ii) The probability of proton or neutron being in high momentum NN SRC is inverse proportional to their relative fractions and can be related to the momentum distribution in the deuteron $n_d(p)$ as:

$$n_{p/n}^A(p) = \frac{1}{2x_{p/n}} a_2(A, y) \cdot n_d(p), \quad (2)$$

where $a_2(A, y)$ is interpreted as a per nucleon probability of finding 2N SRC in the given A nucleus[5–7] and the nuclear asymmetry parameter is defined as $y = |1 - 2x_p|$.

The above two properties are obtained assuming no contributions from pp , nn as well as higher order SRCs. They follow from the assumption that the whole strength of nuclear high momentum distribution as well as per nucleon probability of proton and neutron to be in the SRC is defined by the *same* pn correlation. In Ref.[13] we demonstrated that these properties are seen in the direct calculations using realistic ${}^3\text{He}$ wave function.

Since the SRC is defined by local properties of nuclei, one expects that the A dependence of a_2 , in Eq.(2) is related to the nuclear density, i.e. $a_2(A, y) = a_2(\rho, y)$. This could allow us to estimate the high momentum part of the nucleon momentum distribution not only for finite[13] but also for infinite nuclear matter.

The Parameter a_2 and $A(ee')X$ Processes: In principle, any nuclear process which probes high momentum nucleons in nuclei should allow an extraction of $a_2(A, y)$. One of such processes are high momentum transfer inclusive $A(e, e')X$ reactions measured in special kinematics in which electron scatters off a deeply bound nucleon having large momentum in the nucleus. Two parameters, 4-momentum transfer square $-Q^2$ and Bjorken $x_{Bj} = \frac{Q^2}{2m_N q_0}$ allow us to select these kinematics. Introducing the parameter α , which defines (A times) the light cone momentum fraction of nucleus carried by the interacting nucleon, within impulse approximation:

$$x_{Bj} \equiv \frac{Q^2}{2m_N q_0} = \frac{q_+}{2q_0} \alpha + \frac{q_-}{2q_0} \frac{p_{i+}}{m_N} + \frac{\tilde{m}^2 - m_N^2}{2q_0 m_N} \quad (3)$$

where 4-momentum of the virtual photon is defined as (q_0, q_3) with $q_{\pm} = q_0 \pm q_3$. Also p_{i+} and \tilde{m} represent the “+”-component and mass of the bound initial nucleon. From Eq.(3) in the limit of $Q^2 \gg m_N^2$ such that $\frac{q_-}{q_+} \ll 1$ the condition: $\alpha \approx x_{Bj}$ is satisfied and choosing $x_{Bj} > 1$ will select a nucleon in the nucleus that carries momentum fraction more than that of the stationary nucleon. This observation is the basis of the 2N SRC model[5–7], according to which at $Q^2 \gg m_N^2$ and $1.4 - 1.5 < x_{Bj} < 2$ the interacting nucleon needs to acquire a substantial momentum fraction from the nucleon with which it is in a short-range space-time correlation. The expectation that the γ^*N interaction in SRC will be weakly influenced by the long-range mean-field of A-2 residual nucleus resulted to the prediction of the onset of plateau in the ratios of $A(e, e')X$ and $d(e, e')X$ cross sections at $x_{Bj} > 1.4 - 1.5$ and $Q^2 \gg m_N^2$ [5–7]. First, such plateau was observed in Ref.[7] and later was confirmed in new experiments[8–10] for wide range of nuclei. The measurements also confirmed that the onset of the plateau depends on Q^2 and sets in at $Q^2 \geq 1.5 \text{ GeV}^2$ as it was predicted in the 2N SRC model (see e.g. [5, 6, 11, 14]). It is worth noting that models in which the $x > 1$ cross section is attributed mainly to the final state interaction of the struck nucleon with the residual nucleons is in disagreement with the observed plateau and its onset being a function of Q^2 (for detailed discussion of FSI effects see Ref.[12]).

Based on the expectation that $A(e, e')X$ probes 2N SRCs, from Eq.(2) one observes that

$$a_2(A, y) = \frac{2\sigma_{eA}}{A\sigma_{ed}}, \text{ with } \sigma_{eA} = \frac{d\sigma}{dE_{e'}/d\Omega_{e'}} \quad (4)$$

for those values of x_{Bj} and Q^2 that the measured ratio of the cross sections exhibits the plateau.

Extraction of $a_2(A)$: We analyzed the compilation of the world data on inclusive $A(e, e')X$ reactions from Ref.[10, 15]. Only the data for d , ${}^3\text{He}$, ${}^4\text{He}$, ${}^9\text{Be}$, ${}^{12}\text{C}$, ${}^{27}\text{Al}$, ${}^{56}\text{Fe}$, ${}^{64}\text{Cu}$ and ${}^{197}\text{Au}$ nuclei satisfied the criteria of $x_{Bj} \geq 1.5$ and $Q^2 \geq 1.5 \text{ GeV}^2$. We first constructed the data matrix for central Q^2 and x spanning the following values: $Q^2 = 1.75, 2.25, 2.75, 3.25$ and $x_{Bj} = 1.55, 1.65, 1.75$. For each pairs of Q^2, x_{Bj} we averaged the σ_{eA} cross sections and their errors with $\Delta Q^2 = \pm 0.25 \text{ GeV}^2$ and

TABLE I: The results for $a_2(A, y)$

A	y	This Work	Ref.[7]	Ref.[8, 9]	Ref.[10]
${}^3\text{He}$	0.33	2.07 ± 0.08	1.7 ± 0.3		2.13 ± 0.04
${}^4\text{He}$	0	3.51 ± 0.03	3.3 ± 0.5	3.38 ± 0.2	3.60 ± 0.10
${}^9\text{Be}$	0.11	3.92 ± 0.03			3.91 ± 0.12
${}^{12}\text{C}$	0	4.19 ± 0.02	5.0 ± 0.5	4.32 ± 0.4	4.75 ± 0.16
${}^{27}\text{Al}$	0.037	4.50 ± 0.12	5.3 ± 0.6		
${}^{56}\text{Fe}$	0.071	4.95 ± 0.07	5.6 ± 0.9	4.99 ± 0.5	
${}^{64}\text{Cu}$	0.094	5.02 ± 0.04			5.21 ± 0.20
${}^{197}\text{Au}$	0.198	4.56 ± 0.03	4.8 ± 0.7		5.16 ± 0.22

$\Delta x_{Bj} = \pm 0.05$. Along with the averaged cross sections we estimated the average values of relevant kinematic variables, γ for each bin according to:

$$\bar{\gamma} = \sum \frac{\gamma_i \sigma_i}{\delta \sigma_i^2} / \sum \frac{\sigma_i}{\sigma_i^2}. \quad (5)$$

The a_2 is estimated for each Q^2, x_{Bj} bin as:

$$a_2(A, y) = \frac{\sigma_{eA}(x_A, Q_A^2, \theta_{e,A})}{\sigma_{ed}(x_d, Q_d^2, \theta_{e,d})} \cdot R, \quad (6)$$

where $x_{A(d)}$, $Q_{A(d)}^2$ and $\theta_{e,A(d)}$ are average values for nuclei and d defined according to Eq.(5). The factor R uses the theoretical calculation of $d(e, e')X$ reaction[16, 17] to correct for the misalignment of averaged x, Q^2 and θ_e for nuclei A and d in the following form

$$R = \frac{\sigma_{ed}^{th}(Q_d^2, x_d, \theta_{e,d})}{\sigma_{ed}^{th}(Q_A^2, x_A, \theta_{e,A})} \quad (7)$$

where σ^{th} is a model calculation of the cross sections.

The results of a_2 for the above mentioned nuclei are given in Fig. 1 and in Table I together with the previous[7–9] and recent[10] estimates. Our results are somewhat lower than that of Refs.[7–10], and together with Ref.[10] they agree with the earlier indication[7] that a_2 decreases for heaviest nuclei due to larger asymmetry y which is in agreement with the observation of the suppression of nn/pp vs pn SRCs.

Fitting of $a_2(A, y)$: We now use the extracted values of a_2 to fit them in the parametric form:

$$a_2(A, y) = a_2(A, 0)f(y). \quad (8)$$

The justification for the factorization of A and y dependences follows from the fact that the asymmetry dependence of a_2 is due to its proportionality to the number of the pn pairs *per nucleon*. Thus one expects same function $f(y)$ for nuclei with different A .

First, we fit $a_2(A, 0)$ s for symmetric nuclei. However we have only two data points for $a_2(A, 0)$: ${}^4\text{He}$ and ${}^{12}\text{C}$. To be able to fit the $a_2(A, 0)$ s for the range of $A \geq 12$ we use the approximation[5, 6, 11]:

$$a_2(A, 0) = C \int \rho_A^2(r) d^3r \quad (9)$$

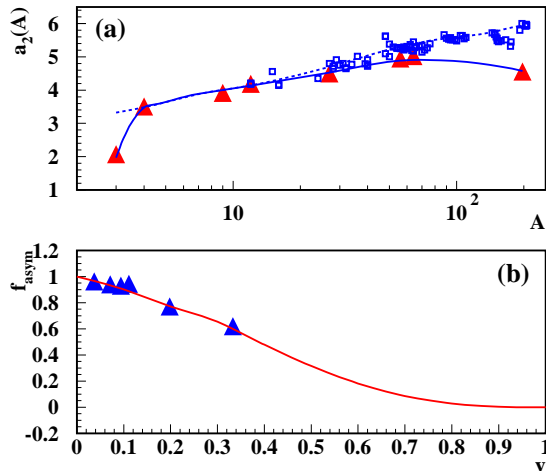


FIG. 1: (a): The A dependence of a_2 . The triangles are the extracted values of a_2 , squares - scaled $\langle \rho_A^2 \rangle$ (see the text), dashed line - $a_2(A, 0)$, solid line - final fit for $a_2(A, y)$. (b) The y dependence of the asymmetry function.

where $\rho_A(r)$ is the nuclear matter density with $\int \rho_A(r) d^3r = 1$. This relation follows from the proportionality of 2N SRCs of finding two nucleons at the same position which is related to the second order of the nuclear matter density function. The fact that the matter density depends weakly on nuclear asymmetry at large A justifies the use of this ansatz for fitting $a_2(A, 0)$.

We calculated the $\langle \rho_A^2 \rangle \equiv \int \rho_A^2(r) d^3r$ for different nuclei using the ρ_A parameterizations extracted from the experimental measurements of nuclear charge densities[19]. Normalizing the calculation of $\langle \rho_A^2 \rangle$ for ^{12}C to the extracted $a_2(12)$ from Table I yields.

$$C = 49.1 \pm 2.6. \quad (10)$$

The $a_2(A, 0)$ "data", generated in this way are presented in Fig.1. Combining these $a_2(A, 0)$ s with the extracted $a_2(^4\text{He})$ (Table I), we then fit $a_2(A, 0)$'s for the whole range of A as it is presented in Fig.1(a)(dashed line).

Next, we use the $a_2(A, 0)$ fit and Eq.(8) to extract the six data points for $f(y)$ from the measured a_2 's for asymmetric nuclei (Fig.1(b)). To be able to make a meaningful fit we supplement these points with the following conditions that have transparent physics interpretations: (a) positiveness condition, $f(y) \geq 0$ for any y ; (b) boundary condition, $f(0) = 1$ and $f(1) = 0$, where the second condition follows from the approximation in which we neglected pp and nn SRCs; (c) since the $\Delta y \rightarrow 0$ limit is valid only in the case of $A \rightarrow \infty$ one obtains that $f'(0) = f'(1) = 0$. The general ansatz for $f(y)$ with minimal number of free parameter satisfying conditions (a)–(c) can be presented in the following form

$$f(y) = (1 + (b - 3)y^2 + 2(1 - b)y^3 + by^4)F(y), \quad (11)$$

where the additional correction function $F(y)$ accounts for the non-smoothness of the asymmetry curve at $y < 0.15$. The best fit is obtained for $b \approx 3$. Combining $a_2(A, 0)$ and $f(y)$ fits in Eq.(8) we obtain the final fit which is the solid line in Fig.1(a).

Extrapolation to Infinite and Superdense Nuclear Matter: The obtained fit in Eq.(8) allows us to estimate $a_2(A, y)$ for infinite nuclear matter since Eq.(9) converges at $A \rightarrow \infty$ and $f(y)$ is finite by definition. The estimate for the symmetric nuclear matter at saturation densities ρ_0 can be obtained using the relation between the nuclear radius and A , $R = r_0 \cdot A^{1/3}$, which yields

$$\langle \rho^2 \rangle_{sym}^{INM} = \frac{1}{A} \int \rho_{A, sym}^2(r) d^3r = \frac{4\pi}{3} \rho_0^2 r_0^3 \approx 1.4 \text{ fm}^{-3}, \quad (12)$$

where we use $\rho_0 = 1.6 \text{ fm}^{-3}$ and $r_0 = 1.1 \text{ fm}$. From Eqs.(8) and (10) we obtain for symmetric nuclear matter at saturation density:

$$a_2(\rho_0, 0) \approx 7.03 \pm 0.41, \quad (13)$$

which is quantitatively in agreement with the a_2 estimated from the y scaling analysis of the $A(e, e')X$ data extrapolated to infinite nuclear matter[20] which yields[21] $a_2 \approx 8.0 \pm 1.24$. Note that our estimate gives the lower limit for a_2 due to the neglect of the nn and pp SRCs.

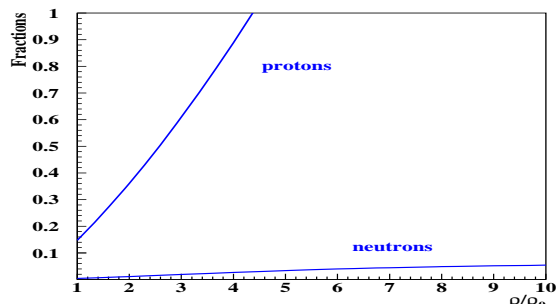


FIG. 2: Density dependence of the fraction of off-Fermi-shell nucleons in $x_p = \frac{1}{9}$ matter.

Next we consider asymmetric nuclear matter. We combine Eqs.(12) and (11) into Eq.(8) to estimate $a_2(\rho, y)$ for given values of nuclear density and asymmetry y . As an example of the application of $a_2(\rho, y)$, we estimate the fraction $P_{p/n}$ of off-Fermi-shell nucleons in the β equilibrium $e - p - n$ superdense asymmetric nuclear matter using the relation (see Eq.(2):

$$P_{p/n}(A, y) = \frac{1}{2x_{p/n}} a_2(A, y) \int_{k_F}^{\infty} n_d(p) d^3p. \quad (14)$$

For the asymmetry y , in our estimates we use the threshold value of $x_p = \frac{1}{9}$ (corresponding to $y = \frac{7}{9}$) below of which the direct URCA processes:

$$n \rightarrow p + e^- + \bar{\nu}_e, \quad p + e^- \rightarrow n + \nu_e \quad (15)$$

will stop in the standard model of superdense nuclear matter consisting of degenerate protons and neutrons[22]. Estimating the Fermi momenta of protons and neutrons in Eq.(14) with $k_{F,N} = (3\pi^2 x_N \rho)^{1/3}$, in Fig.2 we present the off-Fermi-shell fractions of protons and neutrons as a

function of nuclear density. The most interesting result of these estimates is that in equilibrium pn SRCs move the large fraction of protons above the Fermi-shell: at $3\rho_0$ densities half of the protons will be off-Fermi-shell while at $\rho \gtrsim 4.5\rho_0$ all the protons will populate the high momentum tail of the momentum distribution. The situation however is not as dramatic for neutrons, with only *few%* of neutrons populating the high momentum part of the momentum distribution.

Possible Implications for Nuclei and Neutron Stars: Our main observation is that with an increase of nuclear asymmetry the lesser component become more energetic. This is confirmed[13] by direct calculation of the average kinetic energies of proton and neutron using realistic wave function of 3He , in which case one expects neutrons to be more energetic than protons: $\langle T_n \rangle = 18.4$ MeV and $\langle T_p \rangle = 13.7$ MeV. For nuclei with large $A (\geq 40)$ one expects protons to be more energetic than neutrons, with larger fraction of protons occupying high momentum tail of the momentum distributions. This may have several verifiable implications for large A nuclear phenomena[13].

Our observation may have more dramatic implications for the dynamics of neutron stars. Some of them are:

- *Cooling of a Neutron Star:* Large concentration of protons above the Fermi momentum will allow the condition for Direct URCA processes $p_p + p_e > p_n$ [22] to be satisfied even if $x_p < \frac{1}{9}$. This will allow a situation in which intensive cooling of the neutron stars continues well beyond the critical point $x_p = \frac{1}{9}$ (see also Ref.[11]).

- *Superfluidity of Protons:* Transition of protons to the high momentum tail will smear out the energy gap which will remove the superfluidity condition for the protons.

- *Protons in the Neutron Star Cores:* The concentration of protons in the high momentum tail will result in proton densities $\rho_p \sim p_p^3 \gg k_{F,p}^3$. This will favor an equilibrium condition with "neutron skin" effect in which large concentration of protons populates the core rather than the crust of the neutron star. This and the proton superfluidity condition violation may provide different dynamical picture for generation of magnetic fields in the stars.

- *Isospin locking and the stiff equation of state of the neutron stars:* With an increase in density more and more protons move to the high momentum tail where they are in short range tensor correlations with neutrons. In this case one would expect that high density nuclear matter to be dominated by configurations with quantum

numbers of tensor correlations ($S = 1, I = 0$). In such a scenario protons and neutrons at large densities will be locked in the NN iso-singlet state. This will double the threshold of inelastic excitation from $NN \rightarrow N\Delta$ to $NN \rightarrow \Delta\Delta(NN^*)$ transition thereby stiffening the equation of state which is favored by the recent large neutron star mass observation[23].

Possible Universality of the Obtained Result: Our observation is relevant to any asymmetric two-component Fermi system in which the interaction within each component is suppressed while the mutual interaction between two components is enhanced. It is interesting that the similar situation is realized for two-fermi-component ultra-cold atomic systems[24] but with the mutual s-state interaction[27]. One of the most intriguing aspects of such systems is that in the asymmetric limit they exhibit very rich phase structure with indication of the strong modification of the small component of the mixture[25, 26]. In this respect our case is similar to that of ultra-cold atomic systems with the difference that the interaction between components has a tensor nature.

Limitations and Outlook: Our analysis has several limitations: One is that we neglected the contributions from isotriplet 2N as well as 3N SRCs. Even though the statistical errors in the extraction of a_2 are small (Table I), an additional errors are accumulated due to the fitting procedure, especially for the asymmetry function $f(y)$. We estimate the overall error in the extrapolation procedure at $\sim 30\%$.

Finally, the procedure of extraction and fitting of $a_2(\rho, y)$ can be significantly improved with the new high Q^2 and $x_{Bj} > 1$ experiments covering widest possible range of A and y . The semiinclusive $A(e, e'NN)X$ data will allow an inclusion into the analysis a contribution from pp and nn SRCs. Measurements at $x_{Bj} > 2$ domain will allow also to obtain similar estimates for 3N SRCs. Inclusion of all these effects into the analysis will further increase the magnitude of high momentum fraction of the protons. Thus our present results represent most probably the lower limit of the fraction of off-Fermi shell protons in high density nuclear matter.

We are thankful to Drs. J. Arrington, W. Boeglin, A. Bulgac, L. Frankfurt and M. Strikman for helpful comments and discussions. This work is supported by U.S. Department of Energy grant under contract DE-FG02-01ER41172.

[1] E. Piasetzky, M. Sargsian, L. Frankfurt, M. Strikman and J. W. Watson, Phys. Rev. Lett. **97**, 162504 (2006).
 [2] R. Subedi *et al.*, Science **320**, 1476 (2008).
 [3] M. M. Sargsian, T. V. Abrahamyan, M. I. Strikman and L. L. Frankfurt, Phys. Rev. C **71**, 044615 (2005).
 [4] R. Schiavilla, R. B. Wiringa, S. C. Pieper and J. Carlson, Phys. Rev. Lett. **98**, 132501 (2007).
 [5] L. L. Frankfurt and M. I. Strikman, Phys. Rept. **76**, 215

(1981).
 [6] L. L. Frankfurt and M. I. Strikman, Phys. Rept. **160**, 235 (1988).
 [7] L. L. Frankfurt, M. I. Strikman, D. B. Day and M. M. Sargsian, Phys. Rev. C **48**, 2451 (1993).
 [8] K. S. Egiyan *et al.*, Phys. Rev. C **68**, 014313 (2003).
 [9] K. S. Egiyan *et al.*, Phys. Rev. Lett. **96**, 082501 (2006).
 [10] N. Fomin *et al.*, Phys. Rev. Lett. **108**, 092502 (2012)

- [11] L. Frankfurt, M. Sargsian and M. Strikman, *Int. J. Mod. Phys. A* **23**, 2991 (2008).
- [12] J. Arrington, D. W. Higinbotham, G. Rosner, M. Sargsian, *Prog. Part. Nucl. Phys.* **67**, 898 (2012).
- [13] M. M. Sargsian, arXiv:1210.3280 [nucl-th].
- [14] M. M. Sargsian, *Int. J. Mod. Phys. E* **10**, 405 (2001).
- [15] O. Benhar, D. Day and I. Sick, [arXiv:1104.1196 [nucl-ex]].
- [16] W. Cosyn and M. Sargsian, *Phys. Rev. C* **84**, 014601 (2011).
- [17] M. M. Sargsian, *Phys. Rev. C* **82**, 014612 (2010).
- [18] M. M. Sargsian, *et al.*, *J. Phys. G* **G29**, R1 (2003).
- [19] H. De Vries, C. W. De Jager and C. De Vries, *Atom. Data Nucl. Data Tabl.* **36**, 495 (1987).
- [20] D.B. Day *et al.*, *Phys. Rev. C* **40**, 1011 (1989)
- [21] C. Ciofi degli Atti, E. Pace, G. Salme, *Phys. Rev. C* **43**, 1155 (1991).
- [22] J. M. Lattimer, M. Prakash, C. J. Pethick and P. Haensel, *Phys. Rev. Lett.* **66**, 2701 (1991).
- [23] P. Demorest, T. Pennucci, S. Ransom, M. Roberts and J. Hessels, *Nature* **467**, 1081 (2010).
- [24] Y. Shin, M. W. Zwiernik, C. H. Schunck, A. Schirotzek and W. Ketterle, *Phys. Rev. Lett.* **97**, 030401 (2006).
- [25] A. Bulgac and M. M. Forbes, *Phys. Rev. A* **75**, 031605 (2007).
- [26] A. Bulgac and M. M. Forbes, *Phys. Rev. Lett.* **101**, 215301 (2008).
- [27] We are thankful to A. Bulgac for pointing out this similarity.